Matrix Isolation Infrared Spectroscopic and Theoretical Study of the Reactions of Beryllium Atoms with Methanol

Zhengguo Huang, Mohua Chen, and Mingfei Zhou*

Shanghai Key Laboratory of Molecular Catalysts and Innovative Materials, Department of Chemistry, Fudan University, Shanghai 200433, People's Republic of China

Received: December 29, 2003; In Final Form: February 5, 2004

Laser-ablated beryllium atoms have been reacted with methanol molecules during condensation in excess argon at 12 K. Absorptions due to CH_3OBeH, CH_3BeOH, and $CH_3BeOBeH$ were observed and identified on the basis of isotopic IR studies with $^{13}CH_3OH$, $CH_3{}^{18}OH$, and CH_3OD, as well as quantum chemical calculations. The beryllium atoms were observed to insert spontaneously into the O−H bond of methanol to form the CH_3OBeH molecule, while the C−O bond insertion reaction to give the more stable CH_3BeOH product requires activation energy. The CH_3BeOH or CH_3OBeH molecules could further react with a beryllium atom to form the $CH_3BeOBeH$ molecule.

Introduction

Matrix isolation spectroscopy provides a powerful method for delineating reaction mechanisms by facilitating the isolation and characterization of the reactive intermediates. Previous matrix isolation infrared absorption studies of the reactions of laser-ablated beryllium atoms with water have shown that beryllium atoms inserted into the O−H bonds of water to form the HBeOH and HBeOBeH molecules in solid argon.[1] The reactions of methanol resemble the water reactions, but with one hydrogen atom replaced by a methyl group. Therefore, metal atom insertion into CH_3OH can take place in a C−O, O−H, or C−H bond.

The reactions of metal atoms with methanol have received considerable attention.[2−7] Matrix isolation studies have shown that metal atoms, in general, formed complexes with methanol molecules in solid matrixes. Photoexcitation of the complexes with visible or UV light induced oxidative insertion of the metal atoms into the O−H and/or C−O bonds of methanol. A recent investigation in our laboratory[7] on the reaction of magnesium atoms with methanol in a solid argon matrix has identified the formation of the $Mg(CH_3OH)$ complex. The complex underwent photochemical rearrangement to the methylmagnesium hydroxide (CH_3MgOH) molecule upon ultraviolet−visible irradiation. The CH_3MgOH molecule further reacted with a magnesium atom to form the $CH_3MgOMgH$ molecule.

Recently, the reaction of $CH_4 + BeO \rightarrow Be + CH_3OH$ has been theoretically studied at the G2M(MP2) level.[8] The calculations showed that the $BeO + CH_4$ reaction proceeded by barrierless formation of a CH_4BeO complex followed by isomerization to a CH_3BeOH intermediate. The CH_3BeOH molecule further rearranged through a high barrier to a weakly bound CH_3OHBe complex. The results demonstrated that BeO is a useful catalyst at the initial stage of the conversion of methane to important organic compounds. To our knowledge, no experimental study has been reported on the reactions between CH_4 and BeO or CH_3OH and Be. In this paper, we report a combined matrix isolation FTIR spectroscopic and theoretical investigation on the reactions of beryllium atoms with methanol.

* To whom correspondence should be addressed. E-mail: mfzhou@fudan.edu.cn.

Experimental and Theoretical Methods

The experimental setup for pulsed laser ablation and matrix infrared spectroscopic investigation has been described previously.[9] Briefly, the 1064 nm Nd:YAG laser fundamental (Spectra Physics, DCR 150, 20 Hz repetition rate and 8 ns pulse width) was focused onto the rotating beryllium metal target, and the ablated metal atoms were codeposited with methanol in excess argon onto a 12 K CsI window, which was mounted onto a cold tip of a closed-cycle helium refrigerator (Air Products, model CSW202) for 1 h at a rate of approximately 4 mmol/h. Methanol was subjected to several freeze−pump−thaw cycles to minimize possible atmospheric contamination. The isotopic CH_3OD (Merck, 99%) and $^{13}CH_3OH$ and $CH_3{}^{18}OH$ (99%, Cambridge Isotopic Laboratories) and selected mixtures were used in different experiments. Infrared spectra were recorded on a Bruker IFS113V spectrometer at 0.5 cm^{-1} resolution with a DTGS detector. Matrix samples were annealed at different temperatures, and selected samples were subjected to broad-band irradiation with a 250 W high-pressure mercury arc lamp with the globe removed.

Quantum chemical calculations were performed employing the Gaussian 98 program.[10] The three-parameter hybrid functional according to Becke with additional correlation corrections due to Lee, Yang, and Parr (B3LYP) was utilized.[11,12] Additional comparison ab initio calculations were also done using the second-order Moller−Plesset perturbation theory (MP2) as well.[13] The 6-311++G(d,p) basis sets were used.[14,15] The geometries were fully optimized, the harmonic vibrational frequencies were calculated with analytic second derivatives, and zero-point vibrational energies (ZPVEs) were derived. Transition-state optimizations were done with the synchronous transit-guided quasi-Newton (STQN) method.[16] The intrinsic reaction coordinate IRC method was used to track minimum-energy paths from transition structures to the corresponding minima.[17]

Results and Discussion

The infrared spectra of the reaction products are reported, and the product absorptions will be assigned by consideration of the frequencies, isotopic shifts, and splittings of the observed bands and by comparisons with theoretical frequency calculations.

10.1021/jp038028v CCC: $27.50
Published on Web 03/18/2004

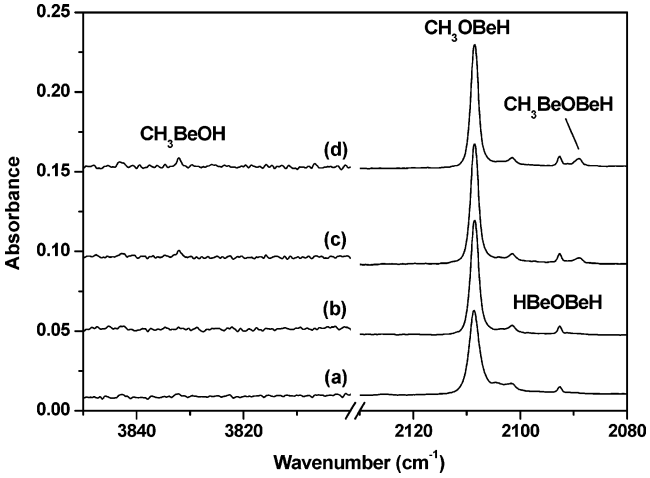

Figure 1. Infrared spectra in the 3850−3800 and 2130−2080 cm^{-1} regions from codeposition of laser-ablated beryllium atoms with 0.1% CH_3OH in argon: (a) 1 h of sample deposition at 12 K, (b) after annealing to 25 K, (c) after 20 min of broad-band irradiation, and (d) after annealing to 30 K.

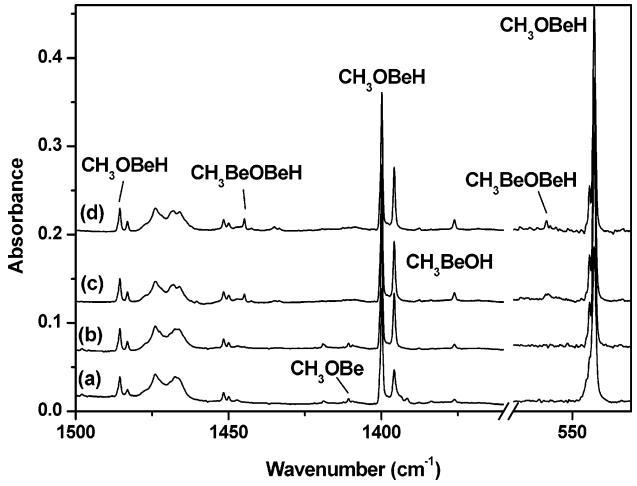

Figure 2. Infrared spectra in the 1500−1360 and 570−530 cm^{-1} regions from codeposition of laser-ablated beryllium atoms with 0.1% CH_3OH in argon: (a) 1 h of sample deposition at 12 K, (b) after annealing to 25 K, (c) after 20 min of broad-band irradiation, and (d) after annealing to 30 K.

Infrared Spectra. Multiple experiments were performed in which laser-ablated beryllium atoms were codeposited with different concentrations of CH_3OH (ranging from 0.05% to 0.2%) in excess argon. These experiments employed relatively low ablation laser energy. Typically, a 5−10 mJ/pulse laser power was used and focused onto a spot of about 0.25 mm^2 on the target. At such experimental conditions, the quantitative metal mole concentrations could not be determined, but were estimated to be less than the CH_3OH concentrations. Condensation of laser-ablated Be atoms with CH_3OH in excess argon at 12 K resulted in partial fragmentation of CH_3OH to CH_2OH (1182.7 and 1047.5 cm^{-1}),[18] H_2CO (1742.1 cm^{-1}), and HCO (1863.4 and 1084.8 cm^{-1}).[19] These fragment absorptions were barely observed with low laser power, but became obvious using relatively high laser power. The infrared spectra in selected regions from codeposition of laser-ablated Be atoms with 0.1% CH_3OH in argon are illustrated in Figures 1 and 2, respectively, and the product absorptions are listed in Table 1. After 1 h sample deposition at 12 K, new product absorptions were observed at 3832.0, 1376.1, 685.4, 683.4, 1410.8, 542.5, 2108.5, 1395.9, 1399.8, 1483.1, and 1485.6 cm^{-1}. The latter two pairs appeared as slightly split doublets. When the matrix sample was annealed to 25 K, the 1410.8 cm^{-1} band decreased, while the 542.5, 2108.5, 1395.9, 1399.8, 1483.1, and 1485.6 cm^{-1} bands increased slightly (about 10%), with little effect on the 3832.0, 1376.1, 685.4, and 683.4 cm^{-1} bands. The 1410.8 cm^{-1} band disappeared on subsequent broad-band irradiation, while the 3832.0, 1376.1, 685.4, and 683.4 cm^{-1} bands markedly increased, and the 542.5, 2108.5, 1395.9, 1399.8, 1483.1, and 1485.6 cm^{-1} bands remained almost unchanged. New absorptions at 2089.0, 1444.8, and 558.5 cm^{-1} also appeared on broad-band irradiation. A subsequent annealing to 30 K had little effect on these absorptions. In addition, weak absorptions due to BeH_2 (2159.6 and 696.7 cm^{-1}),[20] ArBeO (1526.0 cm^{-1}),[21] and HBeOBeH (2092.6 cm^{-1}, reaction product with H_2O presented as a low-level impurity in all the experiments) were also observed.[1]

TABLE 1: Infrared Absorptions (cm^{-1}) from Codeposition of Laser-Ablated Beryllium Atoms with Methanol in Excess Argon

$CH_3{}^{16}OH$	$CH_3{}^{18}OH$	$^{13}CH_3OH$	CH_3OD	assignment
2108.5	2107.2	2108.2	1690.3	CH_3OBeH, ν(Be−H)
1485.6		1485.6		CH_3OBeH, $\delta(CH_3)$
1483.1		1483.1		CH_3OBeH, site
1399.8	1368.3	1387.7	1332.7	CH_3OBeH, ν(Be−O)
1395.9	1363.2	1383.8	1328.8	CH_3OBeH, site
542.5	541.8	542.5	434.2	CH_3OBeH, δ(Be−H)
3832.0	3819.6	3832.0	2798.1	CH_3BeOH, ν(O−H)
1376.1	1363.2	1370.8	1366.6	CH_3BeOH, ν(Be−O)
685.4	685.4	680.4		CH_3BeOH, $\delta(CH_3)$
683.4	683.3	678.8		CH_3BeOH, $\delta(CH_3)$
2089.0	2087.1	2089.0		$CH_3BeOBeH$, ν(Be−H)
1444.8	1413.8	1444.2	1413.2	$CH_3BeOBeH$, ν(Be−O−Be)
558.5	557.6	558.5		$CH_3BeOBeH$, δ(Be−H)
1410.8	1386.5	1399.0	1410.8	CH_3OBe, ν(Be−O)

The experiment was repeated using different laser powers and CH_3OH concentrations. The experiments with higher laser powers gave stronger absorptions. However, the 1410.8, 2089.0, 1444.8, and 558.5 cm^{-1} absorptions were enhanced relative to the others. The experiments with lower laser powers and CH_3OH concentrations gave weaker absorptions. The 542.5, 2108.5, 1395.9, 1399.8, 1483.1, and 1485.6 cm^{-1} bands were weaker on sample deposition, but increased more obviously on annealing (they grew by about 60% on annealing in the experiment with 0.05% CH_3OH and low laser power). The 3832.0, 1376.1, 685.4, and 683.4 cm^{-1} bands were hardly observed on sample deposition, and only appeared on broad-band irradiation.

Experiments were repeated with the $^{13}CH_3OH$, $CH_3{}^{18}OH$, $^{12}CH_3OH + {}^{13}CH_3OH$, $CH_3{}^{16}OH + CH_3{}^{18}OH$, and $CH_3OH + CH_3OD$ samples. The isotopic counterparts of the new product absorptions are listed in Table 1. The infrared spectra in selected regions using different isotopic samples are shown in Figures 3−5, respectively.

Calculation Results. Calculations were performed on the potential reaction products using the B3LYP and MP2 functionals. The optimized geometric parameters are shown in Figure 6, and the vibrational frequencies and intensities are listed in Table 2. The results between the B3LYP hybrid density functional theory and the second-order Moller−Plesset perturbation theory are generally in good agreement. Three $BeCH_3OH$ isomers, namely, the Be(CH_3OH) complex, the inserted methylberyllium hydroxide (CH_3BeOH) and methoxylberyllium hydride (CH_3OBeH) molecules were considered. All three structural isomers were predicted to have a singlet ground state and to be stable with respect to the ground-state reactants: Be + CH_3OH. The geometry and vibrational frequencies of Be(CH_3OH) and CH_3BeOH were recently addressed by Hwang

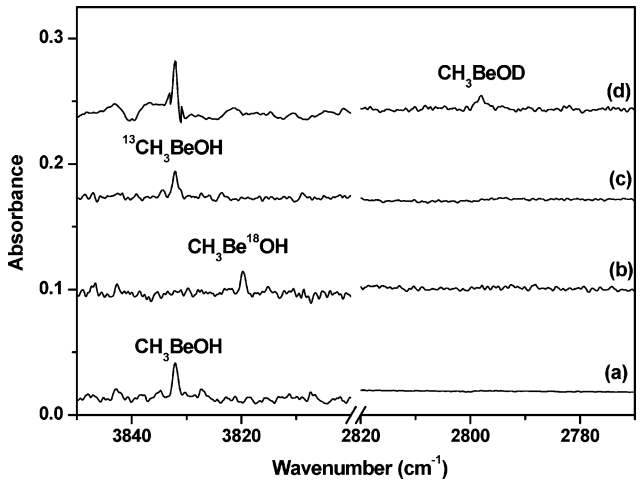

Figure 3. Infrared spectra in the 3850−3800 and 2820−2770 cm^{-1} regions from codeposition of laser-ablated beryllium atoms with different isotopic samples in excess argon. Spectra were taken after annealing to 25 K followed by 20 min of broad-band irradiation. (a) 0.2% CH_3OH, (b) 0.2% $CH_3{}^{18}OH$, (c) 0.2% $^{13}CH_3OH$, and (d) 0.1% CH_3OH + 0.1% CH_3OD.

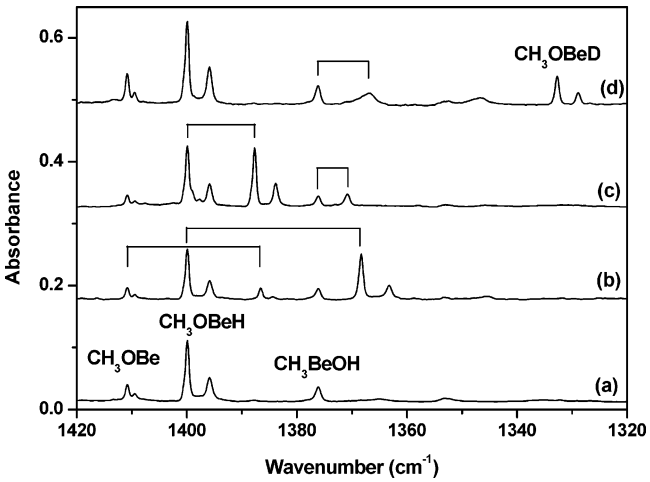

Figure 4. Infrared spectra in the 1420−1320 cm^{-1} region from codeposition of laser-ablated beryllium atoms with different isotopic samples in excess argon. Spectra were taken after annealing to 25 K. (a) 0.2% CH_3OH, (b) 0.1% CH_3OH + 0.1% $CH_3{}^{18}OH$, (c) 0.1% CH_3OH + 0.1% $^{13}CH_3OH$, and (d) 0.1% CH_3OH + 0.1% CH_3OD.

and co-workers at the MP2/6-31G(d,p) level of theory.[8] Our MP2/6-311++G** calculation results on these two molecules are in quite good agreement with previous calculations. The Be(CH_3OH) complex was predicted to have a C_s symmetry with B3LYP, but MP2 calculations predicted a C_1 symmetry. We note that the calculated geometries at the B3LYP and MP2 levels are actually very similar; the only difference is the relative positions of the H atoms in the CH_3 subunit. The binding energy of Be(CH_3OH) with respect to Be + CH_3OH was predicted to be 4.3 kcal/mol at the B3LYP/6-311++G** level after zero-point vibrational energy (ZPVE) and basis set superposition error (BSSE) corrections. This value is slightly higher than the value of 2.6 kcal/mol calculated at the MP2 level. At both levels of theory, the CH_3BeOH molecule was predicted to have a C_s symmetry and the CH_3OBeH molecule a C_{3v} symmetry. The CH_3BeOH molecule is the global minimum and was computed to be about 103.6 (B3LYP) or 103.9 (MP2) kcal/mol lower in energy than the Be(CH_3OH) complex. The CH_3OBeH isomer is 23.9 (B3LYP) or 27.2 (MP2) kcal/mol higher in energy than CH_3BeOH.

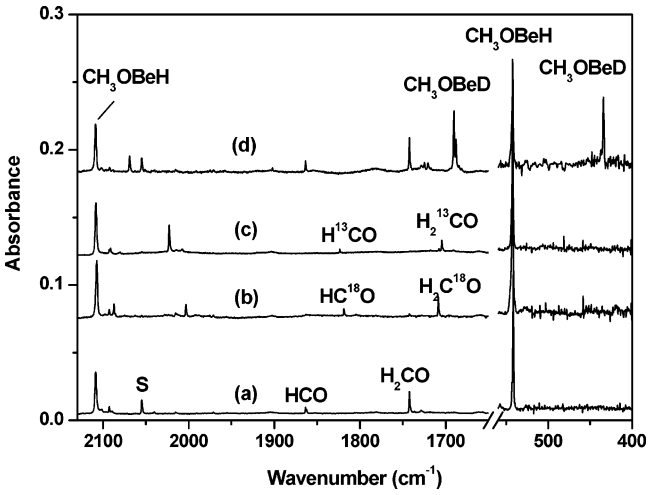

Figure 5. Infrared spectra in the 2130−1650 and 560−400 cm^{-1} regions from codeposition of laser-ablated beryllium atoms with different isotopic samples in excess argon. Spectra were taken after annealing to 25 K. (a) 0.2% CH_3OH, (b) 0.2% $CH_3{}^{18}OH$, (c) 0.2% $^{13}CH_3OH$, and (d) 0.1% CH_3OH + 0.1% CH_3OD. (The 2055 cm^{-1} band which is labeled as "S" is metal independent and presented in all the methanol reaction experiments.)

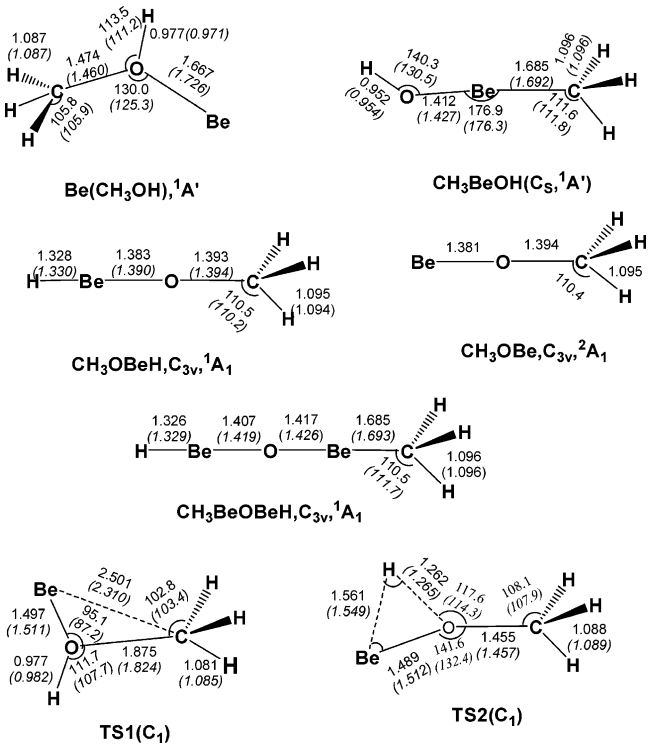

Figure 6. B3LYP/6-311++G** and MP2/6-311++G** (values in parentheses) optimized structures (bond lengths in angstroms, bond angles in degrees) of the potential product molecules and the transition states on the energy profile shown in Figure 7.

Similar calculations were also done on the $CH_3BeOBeH$ and CH_3OBe molecules. The optimized structures are also shown in Figure 6, and the vibrational frequencies and intensities are listed in Table 2.

CH_3OBeH. The bands at 542.5, 2108.5, 1395.9, 1399.8, 1483.1, and 1485.6 cm^{-1} are assigned to the CH_3OBeH molecule. These bands maintained the same relative intensities throughout all the experiments, suggesting different vibrational modes of the same molecule. The 2108.5 cm^{-1} band showed no carbon-13 and oxygen-18 isotopic shift in the $^{13}CH_3OH$ and $CH_3{}^{18}OH$ experiments, but shifted to 1690.3 cm^{-1} with CH_3-

TABLE 2: Calculated Vibrational Frequencies (cm^{-1}) and Intensities (km/mol) of the Reaction Products Shown in Figure 6 at the B3LYP/6-311++G Level**

$Be(CH_3OH)$	3564.3 (320), 3174.4 (2), 3163.6 (6), 3071.4 (14), 1494.5 (12), 1487.3 (3), 1435.0 (13), 1310.6 (46), 1140.3 (1), 1058.0 (38), 880.4 (23),483.5 (30), 255.0 (36), 224.5 (44), 41.9 (0)
CH_3OBeH	3061.0 (43 × 2), 3001.3 (85), 2173.7 (266), 1510.0 (29), 1500.9 (4 × 2), 1417.7 (349), 1191.2 (0.2 × 2), 904.3 (5), 587.5 (199 × 2), 100.7 (5 × 2)
CH_3BeOH	4030.1 (157), 3068.5 (18), 3065.3 (17), 3005.1 (6), 1453.5 (9), 1452.6 (1), 1395.3 (292), 1244.2 (4), 716.5 (76), 714.1 (98), 617.9 (0), 388.9 (198), 269.7 (15), 254.0 (18), 21.4 (155)
CH_3OBe	3064.6 (41 × 2), 3003.9 (84), 1521.4 (108), 1500.2 (5 × 2), 1432.0 (356), 1188.3 (1 × 2), 924.1 (4), 122.2 (9 × 2)
$CH_3BeOBeH$	3067.0 (16 × 2), 3005.4 (6), 2177.2 (264), 1469.5 (682), 1452.8 (1 × 2), 1251.9 (6), 1129.0 (3), 716.0 (105 × 2), 597.9 (195 × 2), 555.3 (0), 292.7 (17 × 2), 92.0 (0.3 × 2)

OD. The band position and the H/D isotopic frequency ratio of 1.2474 indicate that the 2108.5 cm^{-1} band is due to a Be−H stretching vibration. The band position is very close to the analogous modes of HBeOH, HBeOBeH, and BeH_2, which were observed at 2117.7, 2092.6, and 2159.6 cm^{-1}, respectively, in solid argon.[1] In the mixed $CH_3OH + CH_3OD$ spectrum (Figure 5, trace d), only two bands were observed, indicating that only one BeH subunit is involved in the molecule. The 542.5 cm^{-1} band exhibited no isotopic shift with $^{13}CH_3OH$, and a very small (0.7 cm^{-1}) shift with $CH_3{}^{18}OH$, but shifted to 434.2 cm^{-1} with CH_3OD. This band is due to a Be−H bending vibration. The 1399.8 cm^{-1} band is due to a Be−O stretching vibration. It shifted to 1368.3, 1387.7, and 1332.7 cm^{-1} with $CH_3{}^{18}OH$, $^{13}CH_3OH$, and CH_3OD samples, respectively. As shown in Figure 4, the 1399.8 cm^{-1} band split into doublets in the experiments with mixed $CH_3{}^{16}OH + CH_3{}^{18}OH$, $^{12}CH_3OH + {}^{13}CH_3OH$, and $CH_3OH + CH_3OD$ samples, indicating that the molecule contains only one C atom and one O atom. The 1395.9 cm^{-1} band exhibited the same isotopic shifts and splittings as the 1399.8 cm^{-1} band, and is due to site absorption. The 1485.6 and 1483.1 cm^{-1} bands are assigned to the CH_3 deformation mode at two different trapping sites.

The assignment is supported by B3LYP calculations. As listed in Table 2, the four experimentally observed vibrational modes of CH_3OBeH were predicted at 2173.7, 1510.0, 1417.7, and 587.5 cm^{-1}, which require scaling factors (observed frequency/calculated frequency) of 0.970, 0.984, 0.987, and 0.923 to fit the observed values. These four modes were computed to have 266:29:349:398 km/mol relative IR intensities, which is in reasonable agreement with the observed relative integrated band intensities of 0.140:0.035:0.183:0.353. However, besides the above-characterized vibrational modes, the asymmetric and symmetric C−H stretching modes were predicted to have appreciable intensities as well (87 and 85 km/mol IR intensities; see Table 2); these two modes were not observed in the experiments. As has been pointed out,[22−24] DFT calculations do not provide very reliable IR intensity predictions in some cases. It is found that the IR intensities of the vibrations such as C−H stretching are substantially overestimated by DFT calculations. As listed in Table 3, the isotopic frequency ratios calculated for each observed mode are in good agreement with the experimental values, which provide compelling evidence for the identification of the CH_3OBeH molecule.

CH_3BeOH. Absorptions at 683.4, 685.4, 1376.1, and 3832.0 cm^{-1} increased at the same rate on broad-band irradiation, and are assigned to different vibrational modes of the CH_3BeOH molecule on the basis of isotopic substitutions. The 3832.0 cm^{-1} band lies in the region expected for an O−H stretching vibration. This band showed no carbon-13 shift with $^{13}CH_3OH$, but shifted to 2798.1 and 3819.6 cm^{-1} with CH_3OD and $CH_3{}^{18}OH$. The H/D ratio of 1.3695 and $^{16}O/^{18}O$ ratio of 1.0032 are characteristic of an O−H stretching vibration. For example, the analogous modes of CH_3MgOH and HBeOH were observed at 3840.1 and 3841.8 cm^{-1} with about the same $^{16}O/^{18}O$ ratios as the 3832.0 cm^{-1} band.[1,7] In the mixed $CH_3{}^{16}OH + CH_3{}^{18}OH$ and $CH_3OH + CH_3OD$ experiments, only the pure isotopic counterparts were observed, indicating that only one OH is involved in this mode. The 1376.1 cm^{-1} band is due to a Be−O stretching vibration. This band shifted to 1363.2, 1370.8, and 1366.6 cm^{-1} with $CH_3{}^{18}OH$, $^{13}CH_3OH$, and CH_3OD samples, respectively. The 685.4 and 683.4 cm^{-1} bands are due to CH_3 deformation modes. Both bands exhibited very small shifts with $CH_3{}^{18}OH$ (0.0 and 0.1 cm^{-1}) and $^{13}CH_3OH$ (5.0 and 4.6 cm^{-1}).

TABLE 3: Comparison of the Observed and Calculated (B3LYP/6-311++G) Isotopic Frequency Ratios of the Reaction Products**

		$^{16}O/^{18}O$		$^{12}C/^{13}C$		H/D	
molecule	mode	obsd	calcd	obsd	calcd	obsd	calcd
CH_3OBeH	ν(Be−H)	1.0006	1.0005	1.0001	1.0000	1.2474	1.2578
	$\delta(CH_3)$		1.0074	1.0007	1.0000		1.0135
	ν(Be−O)	1.0230	1.0262	1.0087	1.0090	1.0503	1.0529
	δ(Be−H)	1.0013	1.0017	1.0000	1.0000	1.2494	1.2319
CH_3BeOH	ν(O−H)	1.0032	1.0035	1.0000	1.0000	1.3695	1.3708
	ν(Be−O)	1.0095	1.0097	1.0039	1.0024	1.0070	1.0079
	$\delta(CH_3)$	1.0000	1.0003	1.0073	1.0075		1.0006
	$\delta(CH_3)$	1.0001	1.0006	1.0068	1.0072		1.0007
CH_3-BeOBeH	ν(Be−H)	1.0009	1.0003	1.0000	1.0000		1.2773
	ν(Be−O−Be)	1.0219	1.0228	1.0004	1.0009	1.0224	1.0228
	δ(Be−H)	1.0016	1.0027	1.0000	1.0002		1.2160
CH_3OBe	ν(O−Be)	1.0175	1.0205	1.0084	1.0088	1.0000	1.0000

The calculated frequencies at the optimized geometry of CH_3-BeOH provided excellent support for the proposed identification of this molecule. The four observed vibrational modes were computed at 4030.1, 1395.3, 716.5, and 714.1 cm^{-1}, respectively, which require scaling factors of 0.951, 0.986, 0.957, and 0.957 to fit the observed values. All of these four modes were calculated to be intense (Table 2). Equally important, the calculated isotopic frequency ratios are in excellent agreement with the observed values as listed in Table 3.

$CH_3BeOBeH$. Weak bands at 2089.0, 1444.8, and 558.5 cm^{-1} appeared only after broad-band irradiation. These bands were enhanced relative to the CH_3OBeH and CH_3BeOH absorptions in higher laser power experiments, suggesting the involvement of more than one metal atom. The 1444.8 cm^{-1} band shifted to 1413.8 cm^{-1} with $CH_3{}^{18}OH$, and gave an $^{16}O/^{18}O$ isotopic ratio of 1.0219. This ratio is higher than the harmonic ratio of diatomic BeO, 1.0206, suggesting a Be−O−Be stretching vibration. The 2089.0 and 558.5 cm^{-1} bands can be assigned to the Be−H stretching and bending vibrations, which are very close to those of the CH_3OBeH molecule. Accordingly, we assign the 2089.0, 1444.8, and 558.5 cm^{-1} bands to the CH_3-BeOBeH molecule. For comparison, the Be−H stretching, Be−O−Be stretching, and Be−H bending modes of HBeOBeH were reported at 2092.4, 1493.7, and 578.7 cm^{-1}.[1]

The $CH_3BeOBeH$ molecule was predicted to have a $^1A_1$ ground state with C_{3v} symmetry. The Be−H stretching, Be−O−Be stretching, and Be−H bending modes were computed at 2177.2, 1469.5, and 597.9 cm^{-1} (B3LYP), respectively. The calculated isotopic frequency ratios also are in good agreement with the experimental values (Table 3).

CH_3OBe. A weak band at 1410.8 cm^{-1} was observed on sample deposition, decreased on annealing, and disappeared on broad-band irradiation. The band intensity also was enhanced relative to the CH_3OBeH and CH_3BeOH absorptions in higher laser power experiments. The band shifted to 1386.5 cm^{-1} with $CH_3{}^{18}OH$, and to 1399.0 cm^{-1} with $^{13}CH_3OH$. The isotopic $^{16}O/^{18}O$ ratio of 1.0175 and $^{12}C/^{13}C$ ratio of 1.0084 imply that the band is mainly due to a Be−O stretching vibration, but is slightly coupled with another group containing a C atom. In the mixed $CH_3{}^{16}OH + CH_3{}^{18}OH$ and $^{12}CH_3OH + {}^{13}CH_3OH$ spectra (Figure 4), only the pure isotopic counterparts were presented, indicating that only one C atom and one O atom are involved in the mode. This band exhibited no shift when the CH_3OD sample was used, suggesting that the hydroxylic hydrogen atom is not involved in the molecule. We tentatively assign the 1410.8 cm^{-1} band to the CH_3OBe molecule.

The CH_3OBe molecule was calculated to have a $^2A_1$ ground state with C_{3v} symmetry. The Be−O stretching mode was predicted at 1432.0 cm^{-1}, just 21.2 cm^{-1} above the observed value. This mode was predicted to have the largest IR intensity. The carbon isotopic shift was predicted to fit the observed value very well, but the oxygen isotopic shift was predicted to be slightly higher than the observed value (Table 3).

Reaction Mechanism. Previous matrix isolation studies on the reactions of metal atoms with methanol in solid matrixes have shown that the primary reaction, in general, is the formation of the 1:1 metal−methanol complex.[2−7] Complex formation was manifested by the shift of the vibrational frequencies of the CH_3OH subunit. In our recent study on the reaction of magnesium atoms with methanol in solid argon,[7] the $Mg(CH_3OH)$ complex coordinated through the oxygen of CH_3OH to the magnesium atom was formed. The O−H and C−O stretching modes of CH_3OH were red-shifted by the formation of the complex. In the present experiments, no evidence was found for the formation of the $Be(CH_3OH)$ complex. As has been mentioned, the $Be(CH_3OH)$ complex was calculated to be stable with respect to Be (^1S) + CH_3OH ($^1A'$). The complex was predicted to have a quite strong O−H stretching vibration at 3564.3 cm^{-1} (B3LYP).

Cocondensation of laser-ablated beryllium atoms with methanol in excess argon at 12 K resulted in the formation of the CH_3OBeH molecule. The CH_3BeOH molecule also was presented on sample deposition in the experiments with higher laser powers. These two product molecules are formed by the beryllium atom insertion into the O−H and C−O bonds of CH_3OH. The CH_3OBe molecule also was observed on sample deposition. This molecule most likely was formed by the fragmentation of the CH_3OBeH precursor in the gas phase during the cocondensation process. The formation of CH_3OBe + H from the ground-state CH_3OBeH molecule is endothermic by about 90.2 kcal/mol (B3LYP). The CH_3OBeH absorptions increased on annealing, suggesting that the reaction of ground-state beryllium atom with CH_3OH to form CH_3OBeH, reaction 1, requires no activation energy. The reaction of hydrogen atoms with CH_3OBe molecules should be considered as an alternative mechanism to the formation of CH_3OBeH upon annealing. However, the CH_3OBeH absorptions increased more significantly in the experiments with low CH_3OH concentration and low laser power, which suggests that the formation of CH_3OBeH from CH_3OBe plays a minor role as the CH_3OBe absorption was barely observed in the low concentration and low laser power experiments. The CH_3BeOH absorptions increased only on broad-band irradiation, which indicates that the reaction of ground-state beryllium atom with CH_3OH to form CH_3BeOH, reaction 2,

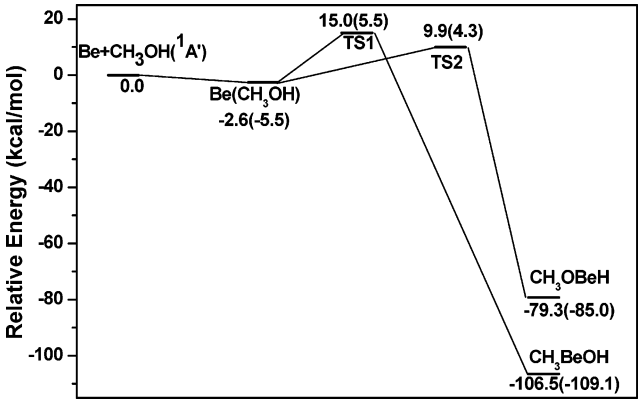

Figure 7. MP2/6-311++G** and B3LYP/6-311++G** (values in parentheses) calculated energy profiles for the reactions of Be + CH_3OH. (Energies are given in kilocalories per mole, and are relative to those of the ground-state reagents.)

$$Be\ (^1S) + CH_3OH\ (^1A') \rightarrow CH_3OBeH\ (^1A_1) \qquad (1)$$

$$Be\ (^1S) + CH_3OH\ (^1A') \rightarrow CH_3BeOH\ (^1A') \qquad (2)$$

requires some activation energy. The observation of CH_3BeOH and CH_3OBeH on sample deposition suggests the participation of excited-state beryllium atoms in the reaction during the cocondensation process. Earlier studies with laser-ablated beryllium have demonstrated the participation of metastable Be ($^3P_1$) in the reactions.[25,26] The excited-state Be is 61 kcal/mol higher in energy than the ground-state Be and likely provides activation energy for the reactions to form CH_3BeOH.

The Be atoms also can insert into the C−H bond of CH_3OH. The C−H bond insertion products were observed in a recent Be + CH_4 study.[27] No C−H bond insertion product was observed in the experiments. The $HBeCH_2OH$ molecule was predicted to lie significantly higher in energy than the CH_3OBeH and CH_3BeOH isomers (43.3 kcal/mol higher in energy than CH_3OBeH at the B3LYP level).

The potential energy profiles of the Be + CH_3OH reactions composed on the basis of calculated relative energies of the products and transition states are shown in Figure 7. The initial step of the Be + CH_3OH reaction is the formation of the $Be(CH_3OH)$ complex, which proceeds without any energy barrier. From the $Be(CH_3OH)$ complex, two reaction paths are considered. One path is the methyl group migration from O to the Be center to form CH_3BeOH via transition state TS1. This process involves the breaking of the C−O bond with the formation of a Be−C bond. The other path proceeds by the hydrogen transfer from O to the Be center to form CH_3OBeH via transition state TS2. This process involves the breaking of the O−H bond and the formation of a Be−H bond. The optimized structures of these transition states are shown in Figure 6. TS1 was predicted to have a C_1 symmetry. The calculated structural parameters at the MP2/6-311++G** level are in agreement with those reported by Hwang and co-workers calculated at the MP2/6-31G(d,p) level.[8] The MP2/6-311++G**-calculated energy barrier at TS1 is 17.6 kcal/mol, and the transition state lies 15.0 kcal/mol higher in energy than the ground-state reactants: Be (^1S) + CH_3OH ($^1A'$). The B3LYP/6-311++G** calculations gave an energy barrier of 11.0 kcal/mol, with TS1 lying 5.5 kcal/mol above the ground-state reactants. The transition state TS2 also was predicted to have a C_1 symmetry, lying 4.3 (B3LYP) or 9.9 (MP2) kcal/mol higher in energy than the

separated reactants, Be (^{1}S) + CH_3OH (^{1}A′), and the energy barrier for the Be(CH_3OH) → CH_3OBeH reaction was estimated to be 9.8 (B3LYP) or 12.5 (MP2) kcal/mol.

The energy profiles shown in Figure 7 indicate that both the C−O and O−H bond insertion reactions are highly exothermic but require activation energy. Although the CH_3BeOH molecule is lower in energy than the CH_3OBeH isomer by about 24.1 (B3LYP) or 27.2 (MP2) kcal/mol, the energy barrier for the formation of CH_3OBeH is lower than that for the formation of CH_3BeOH at both levels of theory. Experimentally, the CH_3OBeH absorptions were observed to increase on annealing, whereas the CH_3BeOH absorptions were increased only on broad-band irradiation. We note that the energy barrier for the formation of CH_3OBeH is low. We expect that the actual energy barrier for this reaction may even be lower than the calculated value; otherwise, a tunnel effect might be responsible for the formation of CH_3OBeH on annealing. The absence of the Be(CH_3OH) complex in the present experiments also implies that the formation of CH_3OBeH requires negligible activation energy.

The CH_3BeOH and CH_3OBeH molecules could further decompose to CH_4 + BeO by hydrogen atom migration. According to recent theoretical studies,[8] the formation of CH_4 + BeO via CH_3BeOH is highly endothermic and proceeds via a transition state lying 81.3 kcal/mol higher in energy than CH_3BeOH. No evidence was found for the formation of the BeO and CH_4 molecules or the $OBeCH_4$ complex in our experiments. However, the $CH_3BeOBeH$ absorptions were produced on broad-band irradiation, suggesting that Be atoms could further insert into the O−H bond of CH_3BeOH or the C−O bond of CH_3OBeH, which were predicted to be exothermic by 91.2 and 115.3 kcal/mol with B3LYP or 103.1 and 130.3 kcal/mol with MP2, respectively. Analogous bimetal insertion products have been observed in previous metal atom and water reactions.[1,28,29]

$$CH_3BeOH\ (^1A') + Be\ (^1S) \rightarrow CH_3BeOBeH\ (^1A_1) \quad (3)$$

$$CH_3OBeH\ (^1A_1) + Be\ (^1S) \rightarrow CH_3BeOBeH\ (^1A_1) \quad (4)$$

The results on the Be + CH_3OH reaction are different from those of the Mg + CH_3OH reaction. In the Mg case,[7] the Mg(CH_3OH) complex was formed, which was rearranged to the C−O bond insertion species CH_3MgOH on broad-band irradiation. The O−H bond insertion product CH_3OMgH was not formed either on annealing or on broad-band irradiation. The B3LYP/6-311++G**-calculated energies showed that both the C−O and O−H bond insertion reactions for Mg require activation energy (31.3 and 32.9 kcal/mol, respectively), and the energy barriers are significantly higher than those of Be. The formations of both CH_3MgOH and CH_3BeOH are photochemical processes, and most likely involve excited-state species.

Conclusions

The reactions of Be atoms with methanol molecules have been investigated with matrix isolation FTIR spectroscopy and theoretical calculations. Cocondensation of laser-ablated Be atoms with methanol in excess argon resulted in the formation of the CH_3OBeH and CH_3BeOH molecules, which were formed by metal atom insertion into the O−H and C−O bonds of methanol. The CH_3OBeH absorptions increased on annealing, indicating that ground-state Be atoms reacted with methanol to form CH_3OBeH spontaneously in solid argon. However, the CH_3BeOH absorptions only were increased upon broad-band irradiation, which suggests that the C−O bond insertion requires activation energy. The CH_3BeOH or CH_3OBeH molecules could further react with beryllium atom to form the $CH_3BeOBeH$ molecule. The aforementioned species were identified via isotopic substitutions as well as theoretical frequency calculations.

Acknowledgment. We greatly acknowledge financial support from the NSFC (Grant 20125033) and the NKBRSF of China.

References and Notes

(1) Thompson, C. A.; Andrews, L. *J. Phys. Chem.* **1996**, *100*, 12214.
(2) Park, M.; Hauge, R. H.; Kafafi, Z. H.; Margrave, J. L. *J. Chem. Soc., Chem. Commun*. **1985**, *1570*.
(3) Maier, G.; Reisenauer, H. P.; Egenolf, H. *Monatsh. Chem.* **1999**, *130*, 227.
(4) Khabashesku, V. N.; Kudin, K. N.; Margrave, J. L.; Fredin, L. *J. Organomet. Chem*. **2000**, *595*, 248.
(5) Lanzisera, D. V.; Andrews, L. *J. Phys. Chem. A* **1997**, *101*, 1482.
(6) Joly, H. A.; Howard, J. A.; Arteca, G. A. *Phys. Chem. Chem. Phys.* **2001**, *3*, *750*.
(7) Huang, Z. G.; Che, M. H.; Liu, Q. N.; Zhou, M. F. *J. Phys. Chem. A* **2003**, *107*, *11380*.
(8) Hwang, D. Y.; Mebel, A. M. *Chem. Phys. Lett*. **2001**, *348*, 303.
(9) Chen, M. H.; Wang, X. F.; Zhang, L. N.; Yu, M.; Qin, Q. Z. *Chem. Phys*. **1999**, *242*, 81. Huang, Z. G.; Zeng, A. H.; Dong, J.; Zhou, M. F. *J. Phys. Chem. A* **2003**, *107*, 2329.
(10) Gaussian 98, revision A.7: Frisch, M. J.; Trucks, G. W.; Schlegel, H. B.; Scuseria, G. E.; Robb, M. A.; Cheeseman, J. R.; Zakrzewski, V. G.; Montgomery, J. A., Jr.; Stratmann, R. E.; Burant, J. C.; Dapprich, S.; Millam, J. M.; Daniels, A. D.; Kudin, K. N.; Strain, M. C.; Farkas, O.; Tomasi, J.; Barone, V.; Cossi, M.; Cammi, R.; Mennucci, B.; Pomelli, C.; Adamo, C.; Clifford, S.; Ochterski, J.; Petersson, G. A.; Ayala, P. Y.; Cui, Q.; Morokuma, K.; Malick, D. K.; Rabuck, A. D.; Raghavachari, K.; Foresman, J. B.; Cioslowski, J.; Ortiz, J. V.; Baboul, A. G.; Stefanov, B. B.; Liu, G.; Liashenko, A.; Piskorz, P.; Komaromi, I.; Gomperts, R.; Martin, R. L.; Fox, D. J.; Keith, T.; Al-Laham, M. A.; Peng, C. Y.; Nanayakkara, A.; Gonzalez, C.; Challacombe, M.; Gill, P. M. W.; Johnson, B.; Chen, W.; Wong, M. W.; Andres, J. L.; Gonzalez, C.; Head-Gordon, M.; Replogle, E. S.; Pople, J. A., Gaussian, Inc., Pittsburgh, PA, 1998.
(11) Becke, A. D. *J. Chem. Phys*. **1993**, *98*, 5648.
(12) Lee, C., Yang, E., Parr, R. G. *Phys. Rev. B* **1988**, *37*, 785.
(13) Moller, C.; Plesset, M. S. *Phys. Rev. B* **1984**, *46*, 618.
(14) McLean, A. D.; Chandler, G. S. *J. Chem. Phys*. **1980**, *72*, 5639.
(15) Krishnan, R.; Binkley, J. S.; Seeger, R.; Pople, J. A. *J. Chem. Phys*. **1980**, *72*, 650.
(16) Head-Gordon, M.; Pople, J. A.; Frisch, M. *Chem. Phys. Lett*. **1988**, *153*, 503.
(17) Gonzalez, C.; Schlegel, H. B. *J. Phys. Chem*. **1990**, *94*, 5523.
(18) Jacox, M. E.; Milligan, D. E. *J. Mol. Spectrosc*. **1973**, *47*, 148. Jacox, M. E. *Chem. Phys.* **1981**, *59*, 213.
(19) Milligan, D. E.; Jacox, M. E. *J. Chem. Phys*. **1969**, *51*, 277.
(20) Tague, T. J., Jr.; Andrews, L. *J. Am. Chem. Soc*. **1993**, *115*, 12111.
(21) Thompson, C. A.; Andrews, L. *J. Chem. Phys*. **1994**, *100*, 8689.
(22) Bauschlicher, C. W., Jr.; Langhoff, S. R. *Spectrochim. Acta, A* **1997**, *53*, 1205.
(23) Lee, Y. K.; Manceron, L.; Papai, I. *J. Phys. Chem. A* **1997**, *101*, 9650.
(24) Miao, L.; Dong, J.; Yu, L.; Zhou, M. F. *J. Phys. Chem. A* **2003**, *107*, 1935.
(25) Thompson, C. A.; Andrews, L.; Davy, R. D. *J. Phys. Chem*. **1995**, *99*, 7913.
(26) Andrews, L.; Chertihin, G. V.; Thompson, C. A.; Dillon, J.; Byrne, S.; Baushlicher, C. W., Jr. *J. Phys. Chem.* **1996**, *100*, 10088.
(27) Greene, T. M.; Lanzisera, D. V.; Andrews, L.; Downs, A. J. *J. Am. Chem. Soc.* **1998**, *120*, 6097.
(28) Kauffman, J. W.; Hauge, R. H.; Margrave, J. L. *High Temp. Sci.* **1984**, *18*, 97. Kauffman, J. W.; Hauge, R. H.; Margrave, J. L. *J. Phys. Chem.* **1985**, *89*, 3541.
(29) Zhou, M. F.; Zhang, L. N.; Shao, L. M.; Wang, W. N.; Fan, K. N.; Qin, Q. Z. *J. Phys. Chem. A* **2001**, *105*, 5801. Zhang, L. N.; Zhou, M. F.; Shao, L. M.; Wang, W. N.; Fan, K. N.; Qin, Q. Z. *J. Phys. Chem. A* **2001**, *105*, 6998.